Ad Hoc Networks 10 (2012) 1306–1321

Contents lists available at SciVerse ScienceDirect

Ad Hoc Networks

journal homepage: www.elsevier.com/locate/adhoc

Energy–delay tradeoff in wireless multihop networks with unreliable links

Ruifeng Zhang [a,c,*], Olivier Berder [a], Jean-Marie Gorce [b], Olivier Sentieys [a]

[a] Université de Rennes 1, IRISA, INRIA, 22300 Lannion, France
[b] Université de Lyon, INRIA, INSA-Lyon, CITI F-69621, France
[c] School of Communication and Info. Engineering, Shanghai University, 200072 Shanghai, China

ARTICLE INFO

Article history:
Received 16 May 2011
Accepted 29 March 2012
Available online 18 April 2012

Keywords:
Energy efficiency
Delay
Unreliable links
Wireless sensor networks
Cross-layer optimization
Multihop networks

ABSTRACT

Energy efficiency and transmission delay are very important parameters for wireless multihop networks. Numerous works that study energy efficiency and delay are based on the assumption of reliable links. However, the unreliability of channels is inevitable in wireless multihop networks. In addition, most of works focus on self-organization protocol design while keeping non-protocol system parameters fixed. While, very few works reveal the relationship between the network performance and these physical parameters, in other words, the best networks performance could be obtained by the physical parameters. This paper investigates the tradeoff between the energy consumption and the latency of communications in a wireless multihop network using a realistic unreliable link model. It provides a closed-form expression of the lower bound of the energy–delay tradeoff and of energy efficiency for different channel models (additive white Gaussian noise, Rayleigh fast fading and Rayleigh block-fading) in a linear network. These analytical results are also verified in 2-dimensional Poisson networks using simulations. The closed-form expression provides a framework to evaluate the energy–delay performance and to optimize the parameters in physical layer, MAC layer and routing layer from the viewpoint of cross-layer design during the planning phase of a network.

1. Introduction

Routing protocols have a significant impact on energy efficiency and latency performances and choosing an efficient routing scheme is a multi-objective optimization problem [1]. Long-hop routes demand substantial transmission power but minimize the energy cost of the reception process, the computation and so on because of the decrease of the number of hops. Meanwhile, long-hop routes are helpful reducing the end to end delay. On the opposite, routes made of shorter hops use less transmission power but maximize the energy cost from the reception process due to an increase in the number of hops. M. Haenggi points out several advantages of using long-hop routing in [2,3], among which high energy efficiency is one of the most important factors. These works reveal the importance of the transmission range and its impact on the energy conservation but do not provide a theoretical analysis on the optimal hop length regarding various networking scenarios.

Some works analyze the optimal transmission range from the viewpoint of physical layer. Chen et al. [4] defines the optimal one-hop length for multihop communications that minimizes the total energy consumption and analyzes the influence of channel parameters on this optimal transmission range in a linear network. The same issue is studied in [5] with a *Bit-Meter-per-Joule* metric where the authors analyze the effects of the network topology, the node density and the transceiver characteristics on the overall energy expenditure. Gao [5] is improved by Deng et al. [6] which shows the effects of network parameters such as node density, network radius on the optimal transmission range and the impacts of the path loss exponent in a 2-dimension Poisson network. Cui et al. [7] solves a cross-layer optimization

* Corresponding author.
E-mail addresses: ruifeng.zhang@irisa.fr (R. Zhang), olivier.berder@irisa.fr (O. Berder), jean-marie.gorce@insa-lyon.fr (J.-M. Gorce), sentieys@irisa.fr (O. Sentieys).

1570-8705/$ - see front matter © 2012 Elsevier B.V. All rights reserved.
http://dx.doi.org/10.1016/j.adhoc.2012.03.012

problem to minimize the energy consumption and the delay for TDMA based small-scale sensor networks.

However, all of the aforementioned works are based on the assumption of a disc link model or a switched link model under which the transmission between two nodes x and x' succeeds if and only if the signal to noise ratio (SNR) $\gamma(x,x')$ at the receiver is above a minimal value γ_{min}. That means perfect reliable links are used for communication and all unreliable links are abandoned. In fact, experiments in different environments and theoretical analyzes in [8–12] have proved that unreliable links have a strong impact on the performance of upper layers such as MAC and routing layers. In our previous work [12], we have shown how unreliable links improve the connectivity of WSNs.

Recently, unreliable links are taken into account in the routing scheme design by introducing a link probability and the effect of link error rate.

In [13], a routing scheme is proposed whose metric for the relay selection is $PRR \times distance$, where PRR stands for Packet Reception Ratio. This routing scheme makes best use of unreliable links to improve the energy efficiency.

These efforts are devoted to the various low-energy routing scheme design while keeping non-protocol system parameters constant, such as the transmission power, transceiver power characteristics, and node density. However, very few works address the relationship between the network performance and the network parameters, in other words, the best network performance that could be obtained by setting all parameters of physical layer, MAC layer and routing layer in a network as a whole.

In [14], we derived the lower bound of the energy–delay tradeoff of opportunistic communications. However, the algorithm for the parameter optimization was not proposed because of the complexity of opportunistic communications. In contrast, thanks to the simplicity, the traditional point to point communications are widely employed in multihop networks, so that its parameter optimization is very practical and important for energy efficiency. Hence, following the analysis method in [14], we focus on the parameter optimization of traditional point to point communications in this paper.

We will explore the Pareto front of the energy–delay tradeoff while adopting a very generic network layer/routing model for low-traffic applications. This Pareto front can serve as a benchmark for preliminary performance evaluation and is suitable in the early phases of network planning and design to optimize physical parameters. To find this bound, a comprehensive energy model is used which includes energy consumption for both data and control packets. Meanwhile a realistic unreliable link model is introduced into the energy model by the metric, *mean energy distance ratio*, $\overline{EDRb}$. We focus on two factors which are tightly related to energy efficiency and delay performance: the *mean hop length* and the *transmission power*.

The contributions of this paper are:

- The closed-form expression of the lower bound of the energy–delay tradeoff for a linear and a Poisson network is achieved in AWGN, Rayleigh fast fading and Rayleigh block fading channels employing both a comprehensive energy model and an unreliable link model.
- The closed-form expressions of the optimal transmission range and the corresponding optimal transmission power are derived in the three aforementioned types of channel.
- The closed form expression of the lower bound of energy efficiency of multihop communication and its corresponding maximum mean delay are obtained.
- The lower bounds of energy–delay tradeoff and energy efficiency are validated by simulations in 2-dimension Poisson networks.
- A parameter optimization process is introduced for the applications with or without a delay constraint.

The rest of this paper is organized as follows: Section 2 concentrates on presenting the models and metrics used in the paper. Section 3 focuses on one-hop transmissions. We derive the lower bounds of energy–delay tradeoff and energy efficiency. Meanwhile, the closed form expressions of optimal transmission range and optimal transmission power are obtained. Section 4 extends the results of one-hop transmissions to the scenario of multihop transmissions. The optimal tradeoff between the energy consumption and the delay in linear networks are achieved. The closed-form expressions of the lower bound in three kinds of channels are provided. In Section 5 simulations are given and analyzed in a 2-dimension network to verify the theoretical results. Then, a parameter optimization process is addressed in Section 6 on the basis of the proposed energy–delay framework. Finally, Section 7 concludes our work.

2. Models and metrics

In this section, we briefly introduce the models and metrics used in this paper. For more details on these models, readers can refer to our previous work [14].

2.1. Energy consumption model

In this paper, we do not consider any specific protocol and assume the corresponding overhead to be negligible. We consider energy efficient nodes, i.e., nodes that only listen to the packets intended to themselves and that send an acknowledgment packet (ACK) to the source node after a correct packet reception. Thus, the energy consumption for the transmission of one packet E_p is composed of three parts: the energy consumed by the transmitter E_{Tx}, by the receiver E_{Rx} and by the acknowledgement packet exchange E_{ACK}:

$$E_p = E_{Tx} + E_{Rx} + E_{ACK}. \tag{1}$$

The energy model for transmitters and receivers [15] are given respectively by:

$$E_{Tx} = T_{start} \cdot P_{start} + \frac{N_{head} + N_b}{R_b \cdot R_{code}} \cdot (P_{txElec} + \beta_{amp} \cdot P_t), \tag{2}$$

and

$$E_{Rx} = T_{start} \cdot P_{start} + \frac{N_{head} + N_b}{R_b \cdot R_{code}} \cdot P_{rxElec}, \tag{3}$$

Table 1
Some parameters of the transceiver energy consumption referring to [16].

Symbol	Description	Value
α	Path-loss exponent ($\geqslant 2$)	3
β_{amp}	Amplifier proportional offset (>1)	14.0
τ_{ack}	ACK ratio	0.08125
B	Bandwidth of channel	250 kHz
f_c	Carrier frequency	2.4 GHz
G_{Tant}	Transmitter antenna gain	1
G_{Rant}	Receiver antenna gain	1
L	Circuitry loss ($\geqslant 1$)	1
N_b	Number of bits per packet	2560
N_{head}	Number of bits of overhead in a packet	0
N_0	Noise level	−150 dBm/Hz
P_{start}	Startup power	38.7 mW
P_{txElec}	Transmitter circuitry power	59.1 mW
P_{rxElec}	Receiver circuitry power	59.1 mW
R_b	Transmission bit rate	250 Kbps
T_{start}	Startup time	0 μs
T_{ACK}	ACK duration	1 ms

where P_t is the transmission power, N_{head} is the number of bit in the overhead of a packet for the synchronization of physical layer, R_{code} is the code rate. The other parameters are described in Table 1.

The energy expenditure model of an acknowledgment is given by:

$$E_{ACK} = \tau_{ack} \cdot (E_{Tx} + E_{Rx}), \tag{4}$$

where

$$\tau_{ack} = \frac{N_{ack} + N_{head}}{N_b + N_{head}} \tag{5}$$

is the ratio between the length of an ACK packet and that of a DATA packet.

As in [14], the energy model for each bit is:

$$E_b = \frac{E_p}{N_b} = E_c + K_1 \cdot P_t, \tag{6}$$

where E_b, E_c and $K_1 \cdot P_t$ are respectively the total, the constant and the variable energy consumption per bit. Substituting (1)–(4) into (6) yields:

$$E_c = (1 + \tau_{ack})\left(\frac{2T_{start} \cdot P_{start}}{N_b} + (1 + \tau_{head})\frac{P_{txElec} + P_{rxElec}}{R_b R_{code}}\right) \tag{7}$$

$$\text{and} \quad K_1 = (1 + \tau_{ack})(1 + \tau_{head})\frac{\beta_{amp}}{R_b R_{code}}, \tag{8}$$

where

$$\tau_{head} = \frac{N_{head}}{N_b}. \tag{9}$$

2.2. Realistic unreliable link model

The unreliable radio link probability (pl) is defined using the packet error rate (PER) [12]:

$$pl(\gamma_{x,x'}) = 1 - \mathrm{PER}(\gamma_{x,x'}) \tag{10}$$

where PER (γ) is the PER obtained from a signal to noise ratio (SNR) γ. And $\gamma_{x,x'}$ is usually defined as [15]:

$$\gamma_{x,x'} = K_2 \cdot P_t \cdot d_{hop}^{-\alpha}, \tag{11}$$

with

$$K_2 = \frac{G_{Tant} \cdot G_{Rant} \cdot \lambda^2}{(4\pi)^2 N_0 \cdot R_s \cdot L}, \tag{12}$$

where d_{hop} is the distance between node x and x', λ is the wavelength, R_s is the symbol rate. Other parameters are presented in Table 1. Note that $R_b = R_s \cdot b$, where b is the modulation order. The unreliable link models are approximated for AWGN and Rayleigh block fading channels respectively as follows (refer to Zhang et al. [17] for more details):

(1) AWGN channels

$$pl_g(\bar{\gamma}) = (1 - 0.1826\alpha_m \cdot \exp(-0.5415\beta_m\bar{\gamma}))^{N_b}, \quad \text{if } \beta_m \cdot \bar{\gamma} \geqslant 2, \tag{13}$$

(2) Rayleigh fast fading channels

$$pl_f(\bar{\gamma}) = \left(1 - \frac{\alpha_m}{2\beta_m\bar{\gamma}}\right)^{N_b}, \tag{14}$$

(3) Rayleigh block fading channels

$$pl_b(\bar{\gamma}) = \exp\left(\frac{-4.25\log_{10}N_b + 2.2}{\beta_m\bar{\gamma}}\right), \quad \text{when } \alpha_m = 1, \tag{15}$$

where α_m and β_m rely on the modulation type and order, e.g., for Multiple Quadrature Amplitude Modulation (MQAM) $\alpha_m = 4(1 - 1/\sqrt{M})/\log_2(M)$ and $\beta_m = 3\log_2(M)/(M-1)$. For BPSK, $\alpha_m = 1$ and $\beta_m = 2$.

2.3. Reliable transmission

Because of the unreliability of propagation channels, retransmission and acknowledgement mechanisms are adopted in this paper to ensure a reliable transmission. According to the derivation in [14], the average number of transmissions needed to ensure a successful reception, $\overline{N}_{tx}$, is computed by:

$$\overline{N}_{tx} = \frac{1}{pl(d_{hop}, P_t)}. \tag{16}$$

2.4. Mean energy distance ratio per bit ($\overline{EDRb}$)

$\overline{EDRb}$ derived in [14] is adopted as the metric of energy consumption. The mean energy consumption per bit for the successful transmission over one hop E_{1hop} including the energy needed for retransmissions is given by $E_{1hop} = E_b(P_t) \cdot \overline{N}_{tx}$.

According to the definition, $\overline{EDRb}$ is formulated as:

$$\overline{EDRb} = \frac{\overline{E}_{1hop}}{d_{hop}} = \frac{E_c + K_1 \cdot P_t}{d_{hop} \cdot pl}. \tag{17}$$

2.5. Mean Delay Distance Ratio ($\overline{DDR}$)

$\overline{DDR}$ is adopted as the metric of mean delay and is obtained by [14]:

$$\overline{DDR} = \frac{D_{hop}\overline{N}_{tx}}{d_{hop}} = \frac{D_{hop}}{d_{hop} \cdot pl}, \tag{18}$$

where D_{hop} is defined as the sum of three delay components:

$$D_{hop} = T_{queue} + T_{tx} + T_{ack}. \tag{19}$$

Here, T_{queue} is the queuing delay during which a packet waits for being transmitted; $T_{tx} = \frac{N_b + N_{head}}{R_b R_{code}}$ is the transmission delay and $T_{ack} = \tau_{ack} \cdot T_{tx}$.

3. Energy–delay tradeoff of one-hop transmissions

This section concentrates on the analysis of the energy–delay tradeoff of one-hop transmissions on the basis of $\overline{EDRb}$ and $\overline{DDR}$ using the analysis method in [14]. According to the definitions of $\overline{EDRb}$ (17) and $\overline{DDR}$ (18), the lower bound of the energy–delay tradeoff of one-hop transmissions can be formulated as:

$$\begin{aligned} &\text{minimize}: \quad \overline{EDRb}(d, P_t) \\ &\text{subject to}: \quad \overline{DDR}(d, P_t) \leqslant ddr, \end{aligned} \tag{20}$$

where ddr is a delay constraint.

3.1. Pareto front of energy–delay tradeoff

According to (11), the transmission distance is related to γ: $d_{hop} = \left(\frac{K_2 P_t}{\gamma}\right)^{\alpha}$. Then, $\overline{EDRb}$ (17) and $\overline{DDR}$ (18) are converted to functions of P_t and γ as follows:

$$\overline{EDRb}(\gamma, P_t) = \frac{E_c + K_1 P_t}{(K_2 P_t)^{\frac{1}{\alpha}}} \cdot g(\gamma) \tag{21}$$

$$\overline{DDR}(\gamma, P_t) = \frac{D_{hop}}{(K_2 P_t)^{\frac{1}{\alpha}}} \cdot g(\gamma) \tag{22}$$

where $g(\gamma) = \frac{\gamma^{\frac{1}{\alpha}}}{pl(\gamma)}$. Note that the initial variables of our optimization problem (d, P_t) have been replaced by γ, P_t. And then, the Pareto front is obtained by simplifying Theorem 1 in [14].

Theorem 1. *The lower bound of the energy–delay tradeoff is provided by the Eqs. (21) and (22) if*

$$\gamma_{opt} = \arg\min_{\gamma} g(\gamma).$$

Proof. Refer to Appendix A in [14]. □

Theorem 1 provides an interesting result that achieving Pareto front is constrained by a constant SNR γ_{opt}:

$$\overline{EDRb}_{opt} = \frac{E_c + K_1 P_t}{(K_2 P_t)^{\frac{1}{\alpha}}} \cdot g(\gamma_{opt}), \tag{23}$$

$$\overline{DDR}_{opt} = \frac{D_{hop}}{(K_2 P_t)^{\frac{1}{\alpha}}} \cdot g(\gamma_{opt}). \tag{24}$$

Note that γ_{opt} is subject to a joint selection (P_{opt}, d_{opt}). Therefore, when a delay constraint ddr is set, according to (24), the optimal transmission power satisfying this delay constraint, P_{opt}, is calculated by:

$$P_{opt} = \frac{1}{K_2}\left(\frac{g(\gamma_{opt}) \cdot D_{hop}}{ddr}\right)^{\alpha}. \tag{25}$$

It is obvious that the optimal transmission power is a monotonic decreasing function with respect to ddr.

Furthermore, the corresponding optimal transmission distance, d_{opt}, is obtained according to (11), as follows:

$$d_{opt} = \left(\frac{K_2 P_{opt}}{\gamma_{opt}}\right)^{\frac{1}{\alpha}} = \frac{g(\gamma_{opt}) \cdot D_{hop}}{\gamma_{opt}^{1/\alpha} \cdot ddr}. \tag{26}$$

Therefore, substituting (25) into (21), the minimum energy consumption under a delay constraint ddr is:

$$\overline{EDRb}_{opt} = E_c \frac{ddr}{D_{hop}} + g(\gamma_{opt})^{\alpha} \frac{K_1}{K_2}\left(\frac{ddr}{D_{hop}}\right)^{1-\alpha}. \tag{27}$$

According to the expression of (27), it can be easily deduced that $\overline{EDRb}_{opt}$ is a convex function with respect to ddr as shown in Fig. 1. Furthermore, note that a lowest point exists in the curve of $\overline{EDRb}_{opt}$—ddr,representing the minimum energy consumption point. On the right of the lowest point, the energy consumption increases with the delay because the transmission power is too small which results to very small hop distance, i.e., the increase of the hop number, which certainly should be avoided in practice. While the curve on the left side of the lowest point is exactly the Pareto front of the energy–delay tradeoff, in other words, the Pareto front is a subset of the lower bound of energy–delay tradeoff. This Pareto front separates the $\overline{EDRb}$—ddr area into two parts: feasible area and infeasible area as shown in Fig. 1. That is to say, the point corresponding to the energy–delay state of a network could exist in the feasible area, but is not possible to access the infeasible area.

Hence, in order to obtain the Pareto front of the energy–delay tradeoff, we need not only the lower bound of energy–delay tradeoff but also the lowest point in the lower bound, i.e., the minimum $\overline{EDRb}$: $\overline{EDRb}_{min}$, and its corresponding ddr, ddr_{max}. We analyze the lowest point in the following subsection.

3.2. Minimal energy point

In this subsection, we derive $\overline{EDRb}_{min}$, ddr_{max} and the corresponding optimal transmission power and distance,

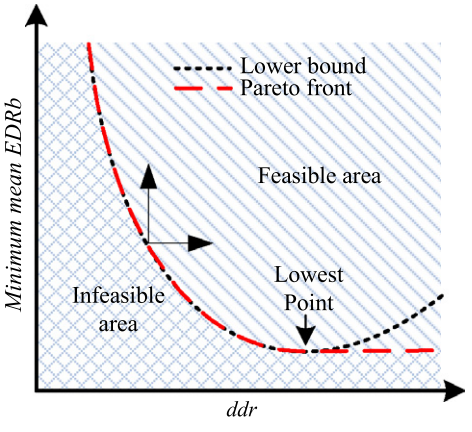

Fig. 1. Lower bound and Pareto front of the energy–delay tradeoff.

because these parameters are very important for delay-tolerant applications.

Through Lagrange method, letting $\frac{\partial \overline{EDRb}_{opt}}{\partial ddr} = 0$, we obtain:

$$\overline{EDRb}_{min} = g(\gamma_{opt}) \frac{\alpha E_c}{\alpha - 1} \left(\frac{K_1(\alpha - 1)}{E_c K_2} \right)^{\frac{1}{\alpha}}, \tag{28}$$

and its corresponding *ddr*:

$$ddr_{max} = g(\gamma_{opt}) D_{hop} \left(\frac{K_1(\alpha - 1)}{E_c K_2} \right)^{\frac{1}{\alpha}}. \tag{29}$$

Note that $\overline{EDRb}_{min}$ provides the lower bound of energy efficiency of a system.

3.2.1. Energy-optimal transmission power P_0

Substituting (29) into (24), we obtain the minimum optimal transmission power:

$$P_0 = \frac{E_c}{K_1(\alpha - 1)}. \tag{30}$$

Substituting (7) and (8) into (30) yields:

$$P_0 = \frac{P_{start}}{\beta_{amp}(\alpha - 1)} \times \frac{2T_{start}}{\frac{N_b + N_{head}}{R_b R_{code}}} + \frac{P_{txElec} + P_{rxElec}}{\beta_{amp}(\alpha - 1)}, \tag{31}$$

where $\frac{N_b + N_{head}}{R_b R_{code}}$ is the transmission duration of a packet. Since $\frac{N_b + N_{head}}{R_b R_{code}} \gg T_{start}$ generally, the first part of (31) can be neglected. Thus, we get:

$$P_0 \approx \frac{P_{txElec} + P_{rxElec}}{\beta_{amp}(\alpha - 1)}. \tag{32}$$

According to (32), it should be noted that P_0 is independent of $pl(\gamma)$ and consequently independent of the modulation and the type of channel. Based on this result, for delay-tolerant applications, we can set the transmission power of a node according to (32) to minimize the total energy consumption, no matter what kind of modulation is used and in what type of channel. Moreover, P_0 provides a threshold of transmission power under which a node will be running in an inefficient state such as the right side curve of the lowest point as shown in Fig. 1.

Furthermore, (32) shows that the characteristics of the amplifier have a strong impact on P_0. When the efficiency of the amplifier is high, i.e., $\beta_{amp} \to 1$, P_0 reaches its maximum value, so that long-hop routes should be used. It coincides with the result of [18]. Meanwhile, it is clear that when the environment of transmission deteriorates, namely, α increases, P_0 decreases meaning that short-hop routes should be adopted.

3.2.2. Energy-optimal transmission range d_0

When P_0 and γ_{opt} are given, the corresponding transmission distance, d_0, may be calculated according to (11), as follows:

$$d_0 = \left(\frac{K_2 P_0}{\gamma_{opt}} \right)^{\frac{1}{\alpha}} = \left(\frac{K_2 E_c}{K_1 \cdot \gamma_{opt} \cdot (\alpha - 1)} \right)^{\frac{1}{\alpha}}. \tag{33}$$

4. Energy–delay tradeoff of multihop transmissions

In this section, we extend the results of the one-hop transmission case developed in Section 3 to the scenarios of multihop transmissions. Meanwhile, the closed-form expressions of lower bound of energy–delay tradeoff are derived in different kinds of channels.

The lower bound of energy–delay tradeoff of a multihop transmission can be abstracted as an optimization problem:

$$\begin{aligned} &\text{minimize :} \quad \overline{E}_{tot}, \\ &\text{subject to :} \quad \overline{D}_{tot} = \text{delay constraint}, \end{aligned} \tag{34}$$

where $\overline{E}_{tot}$ and $\overline{D}_{tot}$ are respectively the end to end energy consumption and delay between the source and destination nodes. To solve this optimization problem, two related theorems about energy and delay are firstly introduced.

4.1. On the optimality of a uniform repartition

Theorem 2. *In a homogeneous linear network, a source node x sends a packet of N_b bits to a destination node x′ using n hops. The distance between x and x′ is d, and the path-loss exponent is greater than 2, $\alpha \geqslant 2$. The length of each hop is $d_1, d_2, \ldots, d_n$ respectively and the average EDRb of each hop is denoted as $\overline{EDRb}(d_i)$ where $i = 1, \ldots, n$. The minimum mean total energy consumption $\overline{Etot}_{min}$ is obtained if and only if $d_1 = d_2 = \cdots = d_n$:*

$$\overline{E}tot_{min} = d \times N_b \times \overline{EDRb}(d/n). \tag{35}$$

Proof. Refer to Appendix D in [14]. □

Theorem 3. *On the same assumption as Theorem 2, the mean hop delay per meter is referred to as $\overline{DDR}(d_i)$ where $i = 1, \ldots, n$. The minimum mean end to end delay $\overline{Dtot}_{min}$ is given, if and only if $d_1 = d_2 = \cdots = d_n$, by:*

$$\overline{Dtot}_{min} = \overline{DDR}(d/n) \times d. \tag{36}$$

Proof. Refer to Appendix E in [14]. □

Based on Theorems 2 and 3, we conclude that, regarding a pair of source and destination nodes with a given number of hops, the single scenario which minimizes both mean energy consumption and mean transmission delay, corresponds to each hop with uniform distance along a linear path as shown in Fig. 2. As a result, the optimization about energy and delay for a single hop will bring the optimization of the same performance for the multihop transmission. Hence, the optimization problem (34) can be converted to the problem (20). Consequently, minimizing energy and delay in a multihop transmission can be achieved by finding the best couple of parameters (d_{opt}, P_{opt}) for a one-hop transmission. In other words, the results obtained in Section 3 can be extended directly to the case of multihop transmissions.

As analyzed above, when $g(\gamma_{opt})$ is obtained, the Pareto front and the lower bound of the energy–delay tradeoff and the lower bound of energy efficiency are achieved at

the same time. In order to obtain γ_{opt} and $g(\gamma_{opt})$, solving $\frac{\partial g(\gamma)}{\partial \gamma}=0$, we get:

$$\gamma_{opt}=\frac{pl(\gamma_{opt})}{\alpha pl'(\gamma_{opt})} \tag{37}$$

where $pl'(\cdot)$ is the first derivation of $pl(\cdot)$. (37) shows that γ_{opt} depends on the kind of channel. In the following subsection, how to obtain γ_{opt}, $g(\gamma_{opt})$ and the Pareto front of energy–delay tradeoff in different channels is presented.

4.2. Pareto front of the energy–delay tradeoff in specific channels

In this subsection, the lower bound of energy–delay tradeoff and the minimum energy point are analyzed in AWGN, Rayleigh fast fading and Rayleigh block fading channels and a general solution is given for the other scenarios.

4.2.1. AWGN

Substituting (13) into (37) and solving the equation of γ yield:

$$\gamma_{optg}=\frac{-1-\alpha N_b \mathrm{W}_{-1}\left[\frac{-\exp\left(\frac{-1}{\alpha N_b}\right)}{0.1826\alpha_m N_b\alpha}\right]}{0.5415\beta_m\alpha N_b}, \tag{38}$$

where $\mathrm{W}_{-1}[\cdot]$ is the branch of the Lambert W function satisfying $\mathrm{W}(x)<-1$ [19]. Substituting (38) into (25) and (26) respectively, we have P_{opt} and d_{opt} in AWGN channels under a delay constraint ddr as follows:

$$\begin{aligned}P_{optg}&=\left(\frac{D_{hop}}{ddr}\right)^{\alpha}\left(1-0.1826\alpha_m\exp\left(\frac{1}{\alpha N_b}+\mathrm{W}_{-1}\left[\frac{-\exp\left(\frac{-1}{\alpha N_b}\right)}{0.1826\alpha_m N_b\alpha}\right]\right)\right)^{-\alpha N_b}\\&\times\frac{-1-\alpha N_b \mathrm{W}_{-1}\left[\frac{-\exp\left(\frac{-1}{\alpha N_b}\right)}{0.1826\alpha_m N_b\alpha}\right]}{0.5415\beta_m\alpha N_b K_2}\\&\approx-\frac{1+\alpha N_b \mathrm{W}_{-1}\left[\frac{-\exp\left(\frac{-1}{\alpha N_b}\right)}{0.1826\alpha_m N_b\alpha}\right]}{0.5415\beta_m\alpha N_b K_2}\left(\frac{D_{hop}}{ddr}\right)^{\alpha}\quad\text{when } N_b>100,\end{aligned} \tag{39}$$

and

$$\begin{aligned}d_{optg}&=\frac{D_{hop}}{ddr}\left(1-0.1826\alpha_m\exp\left(\frac{1}{\alpha N_b}+\mathrm{W}_{-1}\left[\frac{-\exp\left(\frac{-1}{\alpha N_b}\right)}{0.1826\alpha_m N_b\alpha}\right]\right)\right)^{-N_b}\\&\approx\frac{D_{hop}}{ddr}.\end{aligned} \tag{40}$$

Meanwhile, the energy-optimal transmission range d_{0g} is obtained by substituting (38) and (30) into (33):

$$d_{0g}=\left(\frac{-0.5415\beta_m K_2 N_b E_c\alpha}{K_1(\alpha-1)\left(1+\alpha N_b \mathrm{W}_{-1}\left[\frac{-e^{\frac{1}{N_b\alpha}}}{0.1826\alpha_m N_b\alpha}\right]\right)}\right)^{\frac{1}{\alpha}}. \tag{41}$$

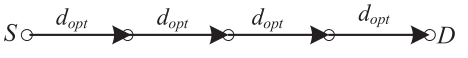

Fig. 2. Equivalent hop distance transmission.

Substituting (38) into (13), we have the optimal link probability in AWGN channels:

$$\begin{aligned}pl_{optg}&=\left(1-0.1826\alpha_m\exp\left(\frac{1}{\alpha N_b}+\mathrm{W}_{-1}\left[\frac{-\exp\left(\frac{-1}{\alpha N_b}\right)}{0.1826\alpha_m N_b\alpha}\right]\right)\right)^{N_b}\\&\approx 1\quad\text{when}\quad N_b>100.\end{aligned} \tag{42}$$

This means that in the optimal configuration, the radio links are reliable.

The lower bound of energy–delay tradeoff according to (27) and its corresponding P_{opt} and d_{opt} in an AWGN channel are shown in Fig. 3 where the related parameters are listed in Table 1. Here, $\gamma_{optg}=9.43$ dB and $pl_{optg}=96.55\%$.

4.2.2. Rayleigh block fading

Substituting (15) into (37) and solving the equation, we obtain:

$$\gamma_{optb}=\frac{\alpha(4.25\log_{10}(N_b)-2.2)}{\beta_m}. \tag{43}$$

Substituting (43) into (25) and (26) respectively, we have P_{opt} and d_{opt} in Rayleigh block fading channel under a delay constraint ddr as follows:

$$P_{optb}=\frac{e\cdot\alpha\cdot(4.25\log_{10}(N_b)-2.2)}{\beta_m K_2}\left(\frac{D_{hop}}{ddr}\right)^{\alpha} \tag{44}$$

and

$$d_{opt_b}=e^{\frac{1}{\alpha}}\frac{D_{hop}}{ddr}. \tag{45}$$

Substituting (43) and (30) into (33) yields:

$$d_{0b}=\left(\frac{\beta_m K_2 E_c}{K_1(\alpha^2-\alpha)(4.25\log_{10}(N_b)-2.2)}\right)^{1/\alpha}. \tag{46}$$

As for the optimal link probability, substituting (43) into (15) yields:

$$pl_{optb}=e^{-\frac{1}{\alpha}}. \tag{47}$$

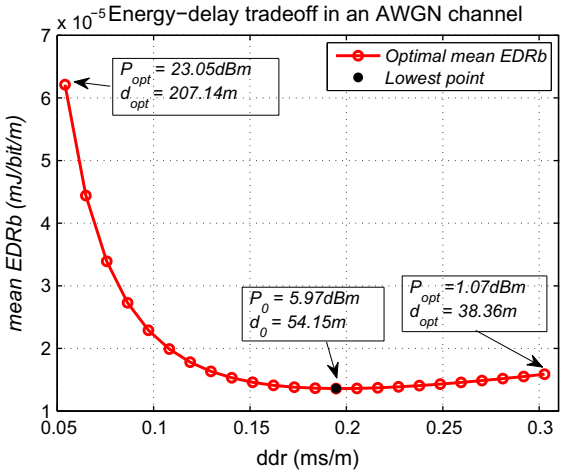

Fig. 3. Theoretical lower bound of the energy–delay tradeoff in an AWGN channel.

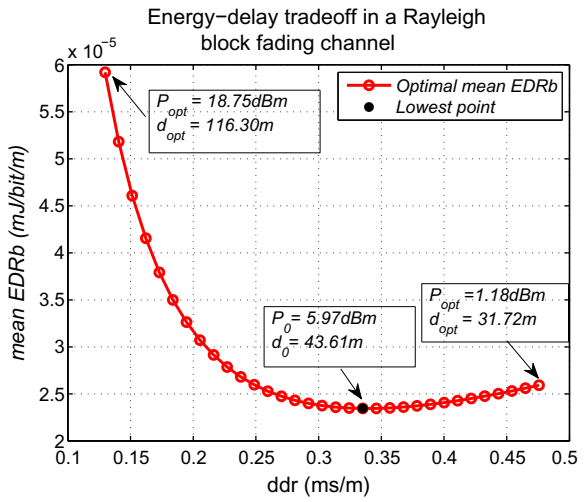

Fig. 4. Theoretical lower bound in of the energy–delay tradeoff in a Rayleigh block fading channel.

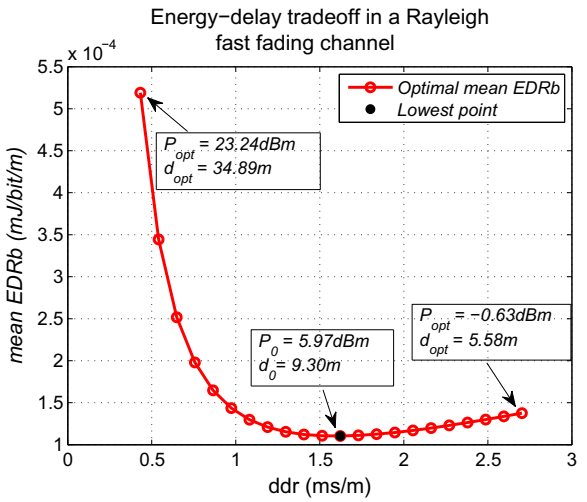

Fig. 5. Theoretical low bound of the energy–delay tradeoff in a Rayleigh fast fading channel.

The lower bound of energy–delay tradeoff according to (27) and its corresponding P_{opt} and d_{opt} in a Rayleigh block fading channel are shown in Fig. 4 where the related parameters are listed in Table 1. Here, $\gamma_{optb} = 12.65$ dB and $pl_{optb} = 71.65\%$.

4.2.3. Rayleigh fast fading

Substituting (14) into (37) and solving this equation, we have:

$$\gamma_{optf} = \frac{\alpha_m(1+\alpha N_b)}{2\beta_m}. \tag{48}$$

Substituting (48) into (25) and (26) respectively, we obtain P_{opt} and d_{opt} in this kind of channel under a delay constraint ddr as follows:

$$P_{optf} = \frac{\alpha_m(1+\alpha N_b)\left(1+\frac{1}{\alpha N_b}\right)^{\alpha N_b}}{2K_2\beta_m}\left(\frac{D_{hop}}{ddr}\right)^{\alpha} \approx \frac{1.359\alpha_m(1+\alpha N_b)}{K_2\beta_m}\left(\frac{D_{hop}}{ddr}\right)^{\alpha} \quad \text{when } N_b > 1 \tag{49}$$

and

$$d_{optf} = \left(1+\frac{1}{\alpha N_b}\right)^{N_b}\frac{D_{hop}}{ddr} \approx \sqrt[\alpha]{2.718}\frac{D_{hop}}{ddr}. \tag{50}$$

Substituting (48) and (30) into (33) as follows:

$$d_{0f} = \left(\frac{2\beta_m E_c K_2}{(\alpha-1)K_1\alpha_m(\alpha N_b+1)}\right)^{\frac{1}{\alpha}}. \tag{51}$$

Meanwhile, the optimal link probability is obtained by substituting (48) into (14) as follows:

$$pl_{optf} = \left(1+\frac{1}{\alpha N_b}\right)^{-N_b} \approx 2.718^{-\frac{1}{\alpha}} \quad \text{when } N_b > 100. \tag{52}$$

The lower bound of the energy–delay tradeoff according to (27) and its corresponding optimal P_{opt} and d_{opt} in a Rayleigh fast fading channel are shown in Fig. 5 where the related parameters are listed in Table 1. Here, $\gamma_{optf} = 32.83$ dB and $pl_{optf} = 71.65\%$.

4.2.4. Other scenarios

Except the above three scenarios, there are a lot of scenarios in which we can not find the closed-form expression of γ_{opt} and $g(\gamma_{opt})$.

The first problem arises when the expression of the link probability is derived but the closed-form expression of γ_{opt} is not obtained. For example, let us consider that the type of channel is Nakagami-m block fading channel ($m \neq 1$) or a coding scheme is employed. In this kind of situation, the sequential quadratic programming (SQP) method in [20] can be adopted to solve the optimization problem of minimizing $g(\gamma)$. Then the exact value of γ_{opt} and $g(\gamma_{opt})$ are obtained. Subsequently, (27) gives the corresponding lower bound of the energy–delay tradeoff.

Another problem is drawn when we are not able to get the expression of the link probability. In this situation, we have to estimate the value of $g(\gamma_{opt})$. According to (22), when P_t is fixed, $g(\gamma_{opt})$ is obtained by minimizing the value of $\overline{DDR}$. Meanwhile, we deduce that $\frac{\overline{DDR}}{D_{hop}} = \frac{1}{pl\times d_{hop}}$ from (18). Hence, the method of finding $g(\gamma_{opt})$ is searching the maximum value of $pl \cdot d_{hop}$. Based on the above analysis, we use two nodes: between them one is assigned as transmitter and the other is assigned as receiver. Then, the following three steps are introduced to find $g(\gamma_{opt})$:

- Set a transmission power, for example, 0 dB.
- Measure the value of $pl \cdot d_{hop}$ for different distances and try to find its maximum value, i.e., max $(pl \cdot d_{hop})$, and recode the corresponding γ.
- Calculate the value of $g(\gamma_{opt})$ through

$$g(\gamma_{opt}) = \frac{(K_2P_t)^{\frac{1}{\alpha}}}{\max(pl \cdot d_{hop})}. \tag{53}$$

So far, the value $g(\gamma_{opt})$ can be obtained in any condition, and the lower bound of the energy–delay tradeoff is

achieved on the basis of (27). The corresponding P_{opt} and d_{opt} are obtained by (25) and (26) respectively, while the corresponding d_0 is obtained by (33).

4.3. Discussions

The energy–delay tradeoff curves reveal the relationship between the transmission power, the transmission delay and the total energy consumption:

(1) For smaller delays (fewer hops), more energy is needed due to the high transmission power needed to reach nodes located far away.
(2) An increased energy consumption is not only triggered by communications with few hops but also arises for communications with several hops where the use of a reduced transmission power leads to too many retransmissions, and consequently wastes energy, too. Hence, the decrease of the transmission power does not always guarantee a reduction of the total energy consumption.
(3) For a given delay constraint, there is an optimal transmission power that minimizes the total energy consumption.

Another point that should be noted is the optimal link probability pl_{opt} in each channel. According to (42), (47) and (52), we easily conclude that the optimal link probability is independent of ddr in each channel, but depends on the type and order of modulation, N_b and α. When $N_b > 100$, the link probability in AWGN channel approximates to 1, which means reliable links are the optimal links to minimize both $\overline{EDRb}$ and $\overline{DDR}$. However, in Rayleigh fast fading and block fading channels, $pl_{optb} = pl_{optf} = 71.65\%$ when $\alpha = 3$, which clearly corresponds to unreliable links. In conclusion, it is helpful to reduce energy consumption by making best use of unreliable links in these two kinds of channels.

To explain the effect of unreliable links on energy efficiency more distinctly, the comparison of energy–delay tradeoff is provided in Fig. 6 under two conditions: optimized link probability and fixed link probability. For the fixed link probability, the BER is set to 10^{-5}, i.e., $pl = 97.47\%$ according to most of works such as [21]. These figures show that, in Rayleigh fast fading and block fading channels, the energy consumption is heavily reduced when the link probability is optimized, i.e., $pl_{opt} = 71.65\%$. However, the energy consumption is almost the same for two conditions in AWGN channels, which verifies our analysis above and indicates the importance of the optimization of link probabilities.

Though the lower bound of the energy–delay tradeoff is derived in linear networks, it will be shown by simulations in Section 5 that this bound is proper for 2-dimensional Poisson distributed networks also.

5. Simulations

The purpose of this section is to verify the theoretical analysis of the lower bounds of the energy–delay tradeoff and the energy efficiency in a 2-dimensional Poisson distributed network by simulations, although these theoretical results are obtained in a linear network.

5.1. Simulation setup

In the simulations, the lower bounds on the energy–delay tradeoff and on $\overline{EDRb}$ are evaluated in an area $\mathscr{A}$ of surface $S_{\mathscr{A}} = 100 \times 1200m^2$ using the simulator Wsnet [22]. The nodes are uniquely deployed according to a Poisson distribution (58).

All the other simulation parameters concerning a node are listed in Table 1. The distance between the source node and the destination node is 1000 m. The source node transmits only one DATA packet of 320 bytes to the destination with BPSK modulation. Relay nodes adopt decode and forward transmission mode and will immediately transmit ACK packet of 26 bytes to the transmitter when receiving the DATA packet correctly. For every hop, the transmitter will retransmit the DATA packet until it is received by the next relay node, that is to say, there is no retransmission limit in order to ensure the reliability. A simulation will be repeated for 2000 times in each different configuration.

The network model used in the simulations assumes the following statements:

- The network is geographical-aware, i.e., each node knows the position of itself and all the neighbor nodes in the simulation network.
- Each node in the simulation network has the same fixed transmission power.
- The nodes sleep when they are not the relay nodes based on a perfect duty cycle scheduling algorithm in order to avoid energy consumption by overhearing.

5.2. Simulations of the energy–delay tradeoff

To verify the lower bound of the energy–delay tradeoff, two routing schemes are used in the simulations: greedy routing [23] and $PRR \times distance$ routing [13], and 802.11 DCF protocol is adopted for MAC layer.

The original greedy routing protocol provides a poor performance on energy efficiency and delay [13], so the optimal transmission distance is employed as the maximum transmission distance of every hop. In addition, in this scope the node closest to the destination node is selected as relay node.

The main idea of $PRR \times distance$ routing protocol is that a source node measures the link probability for each neighbor node using Packet Reception Ratio (PRR). Then, the source node calculates the metric $PRR \times d$ of each node, where d is the distance between the source and its neighbor. Finally, the source selects the node with the maximum value of $PRR \times d$ among all its neighbors in the direction of the destination node. In the simulations, the PRR is computed according to (15) for Rayleigh block fading channel and (13) for AWGN channel.

In the 802.11 DCF protocol, we set the Request to Send (RTS) threshold bigger than the length of DATA packet, i.e.,

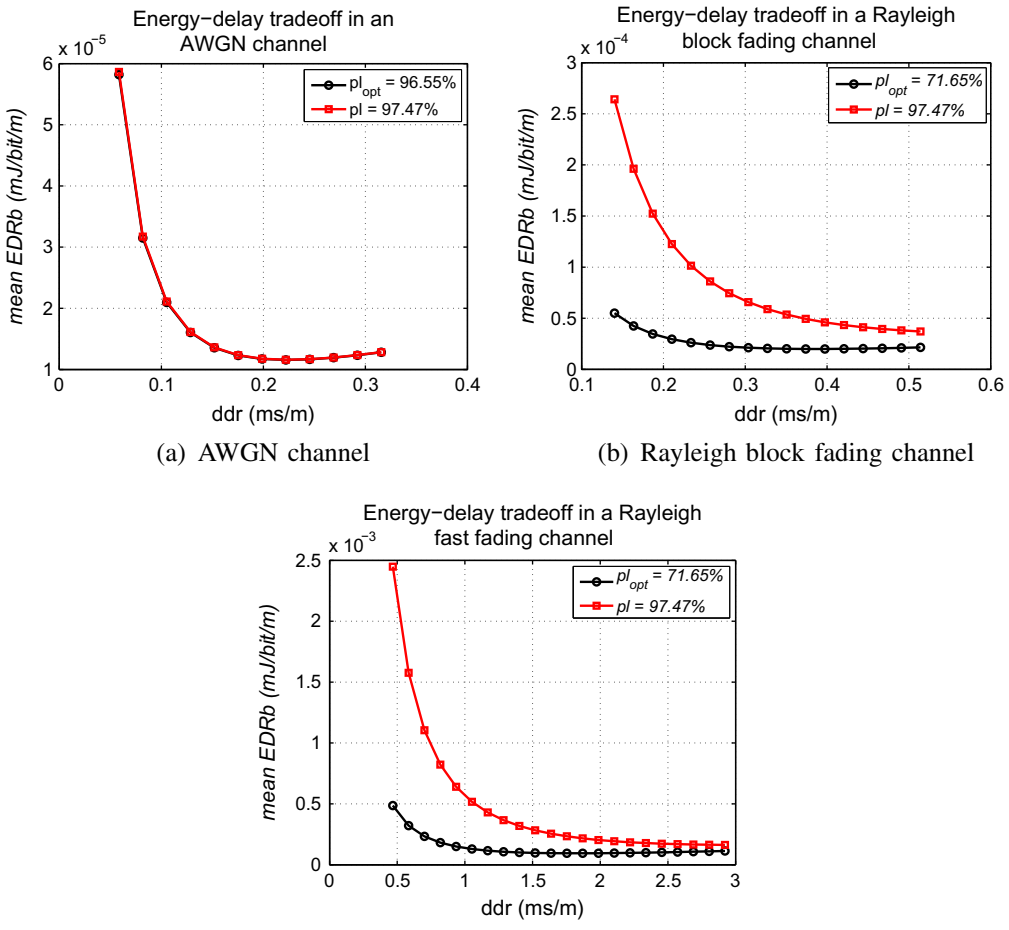

(a) AWGN channel

(b) Rayleigh block fading channel

(c) Rayleigh fast fading channel

Fig. 6. Effect of optimal link probability on the energy–delay tradeoff in different channels.

RTS and CTS will not be sent before the transmission of DATA packet because there is no collision due to the low traffic.

Figs. 7 and 8 provide the simulation results with different node densities in the simulation area compared with the theoretical lower bound of the energy delay tradeoff in an AWGN channel and a Rayleigh block fading channel respectively. These results show that:

(1) *The theoretical lower bound on $\overline{EDRb}$ is adequate for a 2-D Poisson network although its derivation is based on a linear network.*
With the increase of the node density, the simulation result is approaching the theoretical lower bound because relay nodes selected by the routing scheme are more and more near the optimal transmission distance of each hop when the node density increases. We can deduce that the lower bound can be reached when the node density is big enough. Hence, we can conclude that the theoretical lower bound of energy–delay tradeoff is suited to Poisson networks.

(2) *The optimal physical configuration is important to achieve the best network performance.*
When the node density is reduced, theoretical and simulation based curves for the lower bound of the energy–delay tradeoff diverge. In that case, the source node can not find a relay node in the optimal transmission range and has to search for a further or closer relay node, which increases both the energy consumption and the delay.

(3) *Unreliable links play an important role for energy savings in Rayleigh block fading channels.*
In simulations, the mean link probability is 64% for *PRR* × *distance* routing and 73% for greedy routing protocols respectively. Hence, unreliable links also contribute to reach the lower bound on energy–delay tradeoff (as presented in Section 3).

5.3. Simulations of the lower bound of $\overline{EDRb}$

The simulations regarding the lower bound of $\overline{EDRb}$ are also implemented in AWGN and Rayleigh block fading channels. The lowest point of each curve in Figs. 7 and 8

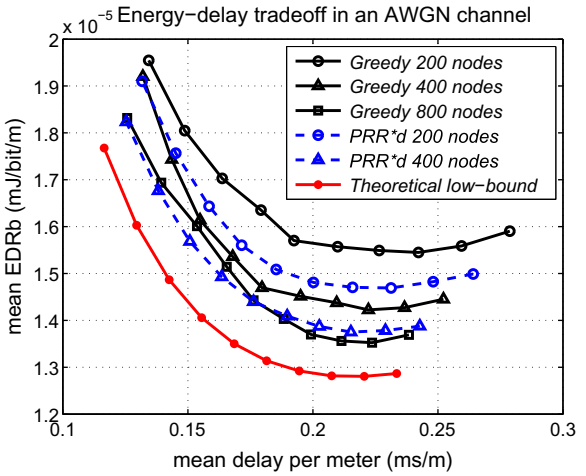

Fig. 7. Simulation results of the energy–delay tradeoff in AWGN channels.

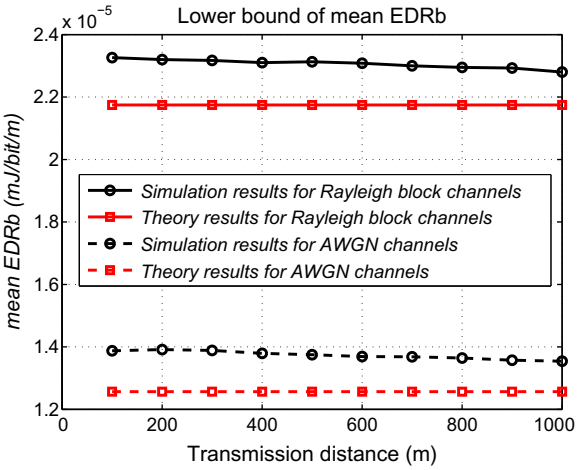

Fig. 9. Lower bound of $\overline{EDRb}$ in different channels for a 400 nodes network.

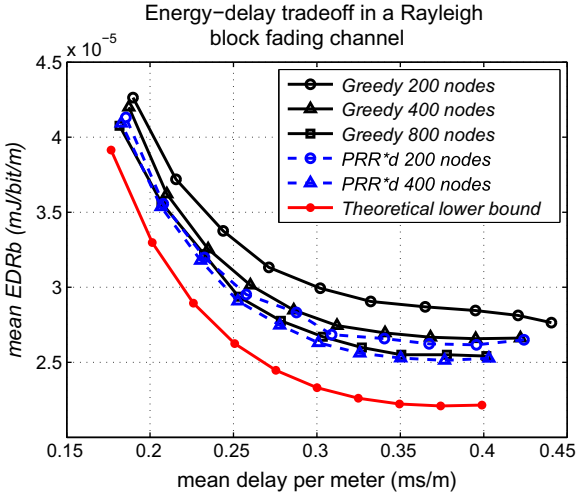

Fig. 8. Simulation results of the energy–delay tradeoff in block fading channels.

corresponds to the most energy efficient point, which reveals that the increase of node density is helpful to let the network performance on energy efficiency achieve the theoretical lower bound.

In Fig. 9, simulation results are given for different transmission distances between the source and the destination nodes. Here 400 nodes are deployed in the simulation area. These results indicate that the theoretical lower bound on the energy efficiency $\overline{EDRb}$ is valid for a Poisson network though its derivation is based on a linear network.

6. Applications of the lower bound of the energy–delay tradeoff

The closed-form expression of the lower bound of the energy–delay tradeoff is obtained in Section 3 and is verified in Section 5 by simulations. In this section, we will explain how to use these results to optimize the parameters in a network.

During the planning phase of a WSN, the first job is to select the hardware platform of nodes to satisfy the performances of a network and other constraints such as the budget. For example, if there are two kinds of hardware, the performance of both kinds of nodes can be directly evaluated using the energy–delay framework proposed in the previous section. These results provide a reference for the hardware selection.

Another important work in the planning phase is to optimize the physical parameters. These parameters include not only node parameters such as the transmission rate, the type and order of modulation, the choice of coding scheme and so on, but also the network parameters such as the node density and protocol parameters such as the number of bits in a data packet and in an ACK packet. we notice that the closed-form expression of the lower bound of the energy–delay tradeoff, (27), includes all parameters of the physical, MAC and routing layers. Therefore, (27) provides a cross-layer framework to both evaluate the energy–delay performance and optimize these parameters. This framework can be used in the following applications:

(1) *Performance evaluation*: During the design or the planning phase of a network, these results about the performance evaluation provide the basis for the choice of sensor nodes and for the choice of routing and MAC layer protocols.
(2) *Benchmark of performance*: Regarding the design of a protocol, the best performance of a network obtained by this framework can act as the benchmark performance in order to measure the performance of a protocol and to adjust its parameters.
(3) *Parameter optimization*: We can optimize parameters such as the transmission power according to the request of performance of a network on the basis of the framework.

In this section, we focus on how to optimize these parameters using this framework. The effect of parameters including physical layer and protocol layer on both $\overline{EDRb}_{opt}$ and $\overline{DDR}_{opt}$ is analyzed. We assume that the transmission power P_t is given. For all the results provided hereafter, the values of physical parameters that are not analyzed are given in Table 1.

6.1. Physical layer parameters

Firstly, on the basis of (21) and (22), the effects of the coding scheme, the modulation order and the transmit rate on the lower bound of the energy–delay tradeoff are studied.

6.1.1. Channel coding

Because $R_{code} < 1$ and $\{E_c, K_1, D_{hop}\} \propto 1/R_{code}$, introducing a coding scheme results in the increase of these parameters. However, coding can reduce the probability of bit or block error and brings the decrease of $g(\gamma_{opt})$. To show the tradeoff of these two contrary effects on $\overline{EDRb}_{opt}$ and $\overline{DDR}_{opt}$, Hamming code (7,4) is used as an example in three kinds of channels.

The results in Fig. 10 indicate that this kind of coding is efficient only in fast fading channel, i.e., code words are spread over different channel states. It even introduces more energy expenditure in AWGN and Rayleigh block fading channels. Therefore, it is the type of channel that decides if a coding scheme should be used.

6.1.2. Transmission rate R_s

In order to investigate the effect of R_s on $\overline{EDRb}$ and $\overline{DDR}$, we first look for their derivatives with respect to R_s:

$$\frac{\partial \overline{EDRb}}{\partial R_s} = \left(\frac{1}{\alpha} - 1\right) R_s^{\frac{1}{\alpha}-2} \times C_{E-Rs}, \tag{54}$$

$$\frac{\partial \overline{DDR}}{\partial R_s} = \left(\frac{1}{\alpha} - 1\right) R_s^{\frac{1}{\alpha}-2} \times C_{D-Rs}, \tag{55}$$

where

$$C_{E-Rs} = \frac{(4\pi)^{\frac{2}{\alpha}} g(\gamma_{opt})(P_{rxElec} + P_{txElec} + P_t \beta_{amp})(1+\tau_{ack})(1+\tau_{head})}{b \cdot R_{code}} \left(\frac{G_{tant} G_{rant} P_t \lambda^2}{LN_0}\right)^{-\frac{1}{\alpha}},$$

$$C_{D-Rs} = \frac{(4\pi)^{\frac{2}{\alpha}} (N_b + N_{head})(1+\tau_{ack}) g(\gamma_{opt})}{b \cdot R_{code}} \left(\frac{G_{tant} G_{rant} P_t \lambda^2}{LN_0}\right)^{-\frac{1}{\alpha}}.$$

It is clear that $C_{E-Rs} > 0$ and $C_{D-Rs} > 0$ and easily deduced that $\frac{\partial \overline{EDRb}}{\partial R_s} < 0$, $\frac{\partial \overline{DDR}}{\partial R_s} < 0$. Thus, $\overline{EDRb}$ and $\overline{DDR}$ are monotonic decreasing functions with respect to R_s. The results in Fig. 11 in the three kinds of channel verify this analysis. Hence, according to this conclusion, the maximum transmit rate that a node can reach should be used in order to minimize both $\overline{EDRb}$ and $\overline{DDR}$ at the price of the increase of the transmission bandwidth.

6.1.3. Modulation

In order to achieve the optimal order of modulation, b_{opt}, we solve $\frac{\partial \overline{EDRb}}{\partial b} = 0$ and $\frac{\partial \overline{DDR}}{\partial b} = 0$, then obtain:

$$b_{opt} = \frac{g(\gamma_{opt})}{g'(\gamma_{opt})\gamma'_{opt}} = \frac{\alpha \cdot \gamma_{opt} \cdot pl(\gamma_{opt})}{\gamma'_{opt}(pl(\gamma_{opt}) - \alpha \cdot \gamma_{opt} \cdot pl'(\gamma_{opt}))}. \tag{56}$$

According to (42), (47) and (52), $pl(\gamma_{opt})$ in the three kinds of channels approximate constant, namely, $pl'(\gamma_{opt}) \approx 0$. Thus,

$$b_{opt} \approx \frac{\alpha \cdot \gamma_{opt}}{\gamma'_{opt}}. \tag{57}$$

On the basis of (57) and γ_{opt} in different channels, we can see that the optimal modulation order is related with only two parameters: α and N_b. In Fig. 12, the numerical results of b_{opt} are shown for the cases of different N_b and α. One should notice that the numerical results in Fig. 12 indicate that the effect of N_b on b_{opt} can be neglected. For example, whatever N_b, the optimal modulation is 16QAM and 64QAM respectively for $\alpha = 2$ and $\alpha = 3$ in a Rayleigh block fading channel. Therefore, the channel path-loss exponent α is the unique factor that has the impact on the optimal order of modulation. Furthermore, we notice that the order of modulation increases with respect to α. Finally, we can conclude that the optimal modulation is obtained when the path-loss exponent and the type of channel are known.

6.1.4. Optimal transmission power

According to the analysis in Section 3, we know that there exists an optimal transmission power (25), when a delay constraint *ddr* is set. When there is no delay request, P_0, obtained by (32), is the optimal transmission power to minimize the total energy consumption. Moreover, P_0 provides a threshold of transmission power under which a node will be running in an inefficient state as described in Section 3. Therefore, the transmission power of each node in a network should not be configured smaller than P_0.

6.2. Protocol layer parameters

6.2.1. Number of bits in an ACK packet N_{ack} and in a header N_{head}

Because $\{K_1, E_c, D_{hop}\} \propto \{N_{ack}, N_{head}\}$,it is easily deduced that the increase of N_{ack} and N_{head} leads to the increment of total $\overline{EDRb}_{opt}$ and $\overline{DDR}_{opt}$ as shown in Fig. 13. Therefore, removing the ACK packet and the packet header could represent a good solution in the viewpoint of energy saving. However, due to the unreliability of wireless links as described in Section 1, a lot of protocols adopt an ACK packet as a feedback mechanism. However A packet header is mandatory for packet synchronization. Consequently, N_{ack} and N_{head} should be reduced as less as possible.

6.2.2. Number of bits in a data packet N_b

Since $\{E_c, K_1\} \propto 1/N_b$,the increase of N_b diminishes E_c and K_1, but enlarges $g(\gamma_{opt})$. Thus, these two contrary effects on $\overline{EDRb}_{opt}$ bring on an optimal number of bits. The results in Fig. 13 validate our analysis in three kinds of channels. Meanwhile, the results in these figures indicate that the increase of N_{ack} and N_{head} leads to the increase of the optimal N_b. For instance, in a Rayleigh block fading channel, $N_{bopt} = 300$ bytes when $N_{ack} = 13$ bytes and

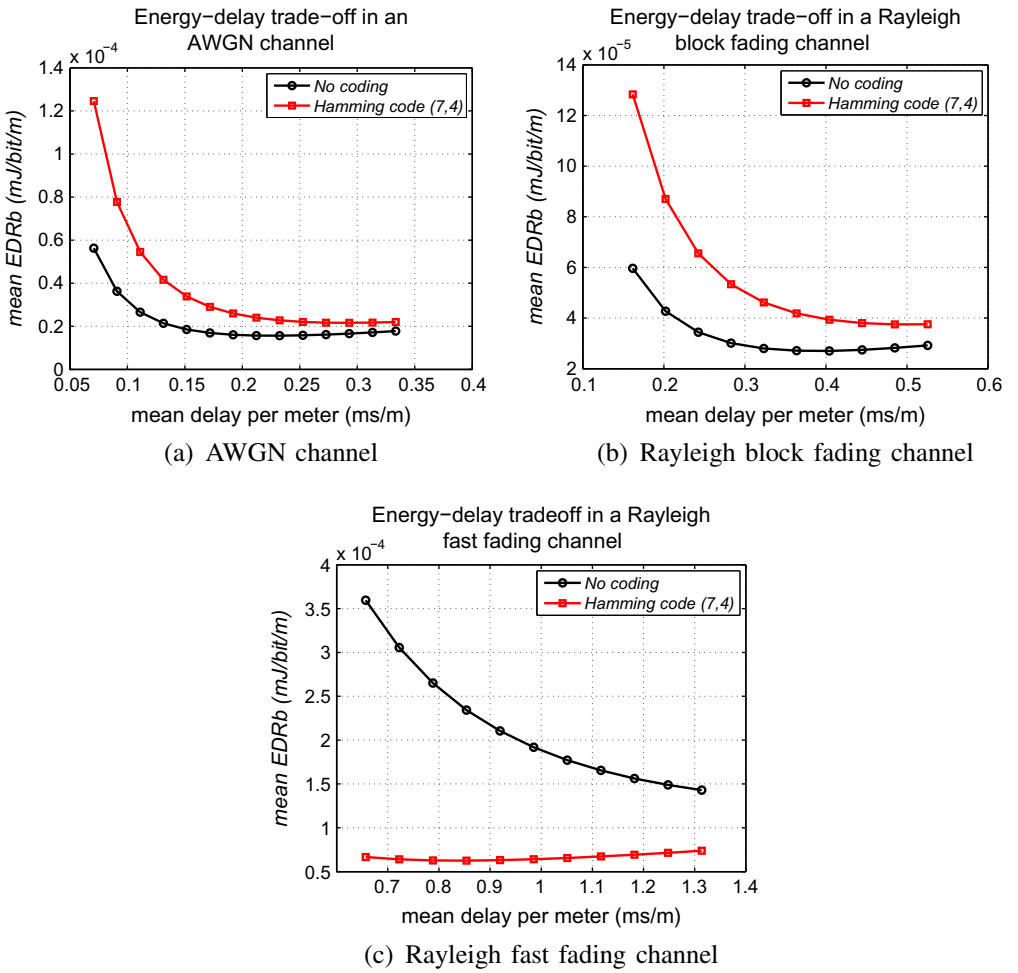

(a) AWGN channel (b) Rayleigh block fading channel

(c) Rayleigh fast fading channel

Fig. 10. Effect of a coding scheme on the energy–delay tradeoff in different channels.

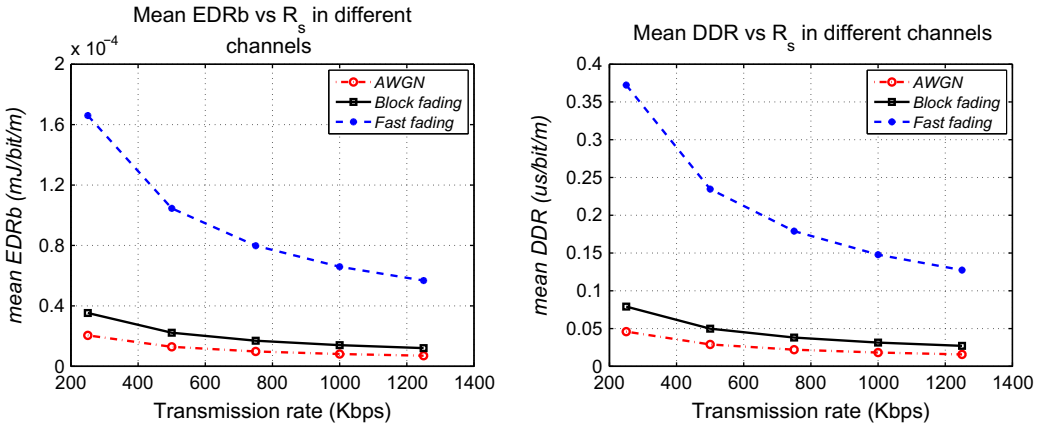

(a) mean EDRb (b) mean DDR

Fig. 11. Effect of transmit rate on the energy–delay tradeoff in different channels.

N_{head} = 2 bytes, while N_{bopt} = 650 bytes when N_{ack} = 28 - bytes and N_{head} = 2 bytes.

In addition, when there is no ACK packet and packet header, N_b should be as small as possible. However, as

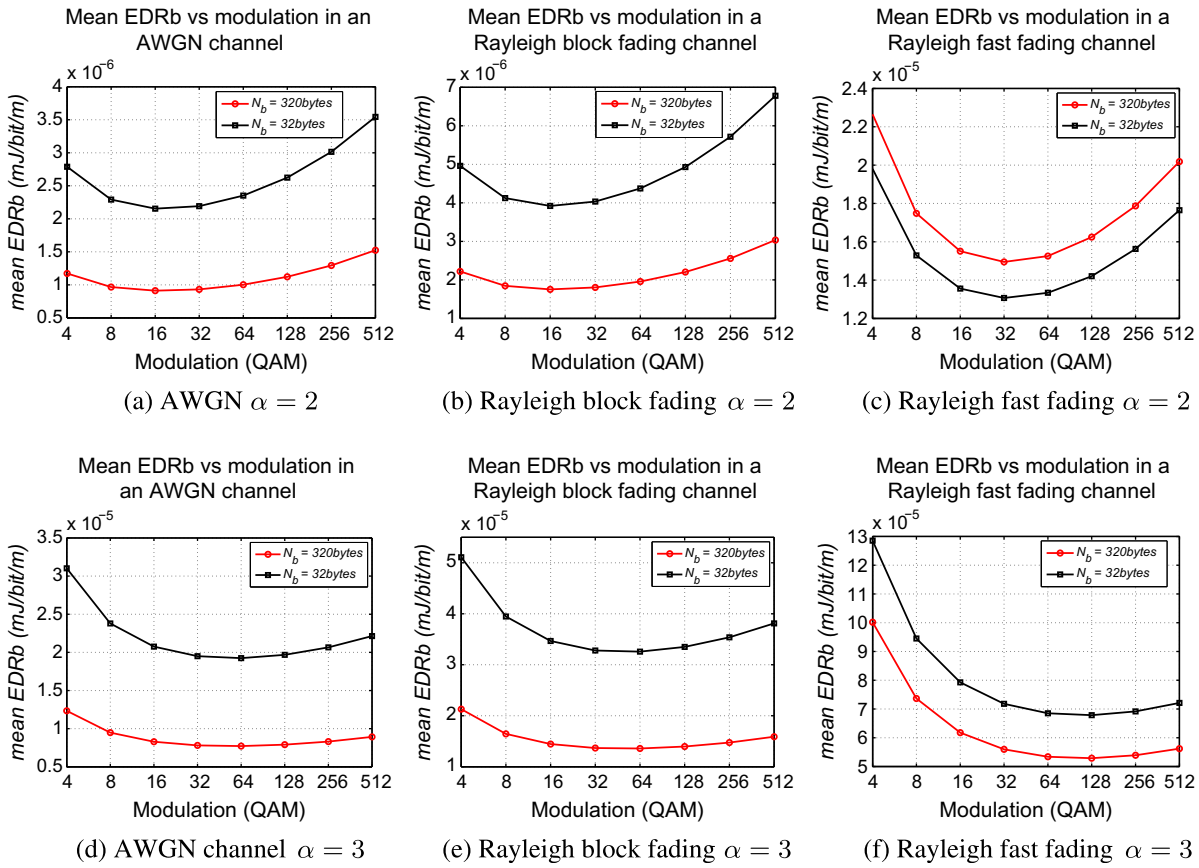

Fig. 12. Effect of modulation on the energy–delay tradeoff in different channels.

mentioned above, an ACK packet and a packet header are necessary for most of cases, thus, we focus on the results with N_{ack} and N_{head}. It should be noticed that the difference of corresponding $\overline{EDRb}_{opt}$ between N_{bopt} and non-optimal N_b is very small especially in AWGN channels and Rayleigh block fading channels, so that the optimization of N_b can be neglected.

Meanwhile, under a *ddr* constraint, the simultaneous increase of N_b leads to the increase of d_{opt} and P_{opt} in the three kinds of channels mentioned, according to (40), (45), (50), (39), (44) and (49). This means a long-hop transmission should be used, which is helpful to reduce the node density of a network. Consequently, N_b can be big properly in order to diminish the cost of a network.

6.2.3. Delay from MAC protocol T_{queue}

According to (18), the increase of T_{queue} will lead to the increment of D_{hop}. It can be deduced that the transmission power should be increased to satisfy the same delay constraint on the basis of (27) and $\overline{EDRb}$ will be increased. The numerical results in Fig. 14 verify the above analysis. This conclusion shows that the process leading to the increase of T_{queue}, such as RTS and CTS should be reduced or removed, to improve the energy efficiency of a network.

Besides the above parameters, the effect of the other parameters such as the strength of fading of a channel or the integration of several parameters can be also analyzed according to the different applications because this framework includes each physical parameter.

6.3. Minimum node density

The node density of a network is tightly related with its total cost. A too high node density not only leads to high cost, but also brings an increase of idle energy which is not considered here. However, a too low node density results to more transmission energy consumption because the distance between two nodes is too long. In this subsection, we discuss how to config the node density according to d_{opt} under a delay constraint *ddr*, or d_0 for the delay-tolerant applications.

Here, we assume a Poisson distributed network according to:

$$P(n \text{ nodes in } S_A) = \frac{(\rho \cdot S_A)^n}{n!} e^{-\rho \cdot S_A}. \tag{58}$$

where S_A is the surface of area A and ρ is the node density.

The relationship between the node density and the expected distance between two nearest nodes, $\bar{d}$, is provided

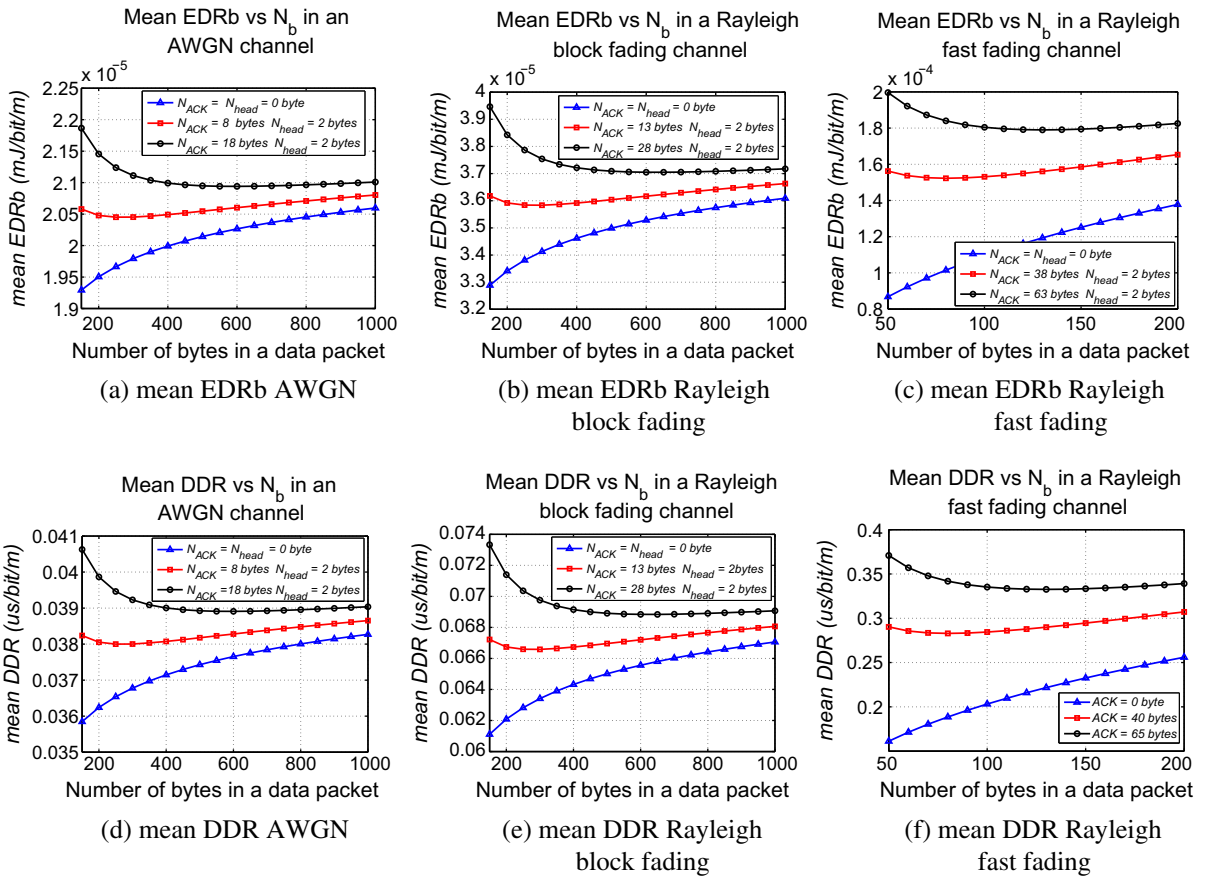

(a) mean EDRb AWGN (b) mean EDRb Rayleigh block fading (c) mean EDRb Rayleigh fast fading

(d) mean DDR AWGN (e) mean DDR Rayleigh block fading (f) mean DDR Rayleigh fast fading

Fig. 13. Effect of N_b on the optimal $\overline{EDRb}$ and $\overline{DDR}$.

in [24] in a 2-dimension Poisson distribution network as follows:

$$\bar{d} = \frac{\sqrt{\pi}}{2\sqrt{\rho\Phi}}, \tag{59}$$

where Φ is the central angle of a circle sector whose center point is a node. According to the previous analysis, we should let $\bar{d} \leqslant d_{opt}$ or $\bar{d} \leqslant d_0$ in order to minimize the energy consumption, so that we have:

$$\rho \geqslant \frac{\pi}{4\Phi\{d_{opt} \text{ or } d_0\}^2}. \tag{60}$$

Finally, on the basis of (60), the minimum node density is obtained to improve the energy efficiency and deduce the transmission latency in a network.

In [25] and [26], the mean distance between two nodes are presented for Manhattan, hypercubes, and shufflenets networks. Using the similar method, the minimum node density can be deduced in these kinds of networks.

6.4. Process of parameters optimization

Integrating the above analysis results, the process of parameter optimization is explained in detail as the following steps:

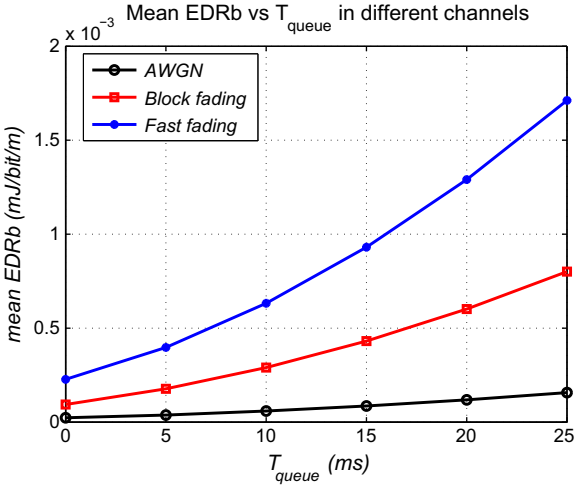

Fig. 14. Effect of T_{queue} on the energy–delay tradeoff in different channels.

(1) The physical parameters of a node should be obtained and E_c, K_1 and K_2 are calculated according to these parameters. Meanwhile, N_{head}, N_{ack} and ddr are obtained according to the protocol using in a network.

(2) R_s is decided according to the maximum limit value of transmission rate of a node.
(3) Select the corresponding N_b according to the application.
(4) The coding scheme is selected according to the type of channel.
(5) The order of modulation is optimized using a searching method based on the framework (27).
(6) Calculate the optimal transmission power P_{opt} according to (25).
(7) Calculate the optimal transmission distance d_{opt} and minimal node density ρ on the basis of (26) and (60) respectively.

7. Conclusions

In this paper, using a realistic unreliable link model, we explored the lower bound of the energy–delay tradeoff and the energy efficiency in AWGN, Rayleigh fast fading and Rayleigh block fading channels. Firstly, we introduced a metric for energy efficiency, $\overline{EDRb}$ and a metric $\overline{DDR}$ for mean delay, which are combined with the unreliable link model. $\overline{EDRb}$ reveals the relation between the energy consumption of a node and the transmission distance which can contribute to determine an optimal route at the routing layer. By optimizing $\overline{EDRb}$ and $\overline{DDR}$, a closed-form expression of the lower bound of energy–delay tradeoff is obtained for these three kinds of channel. Theoretical analysis and simulation results showed that unreliable links in the transmission contribute to improve the energy efficiency of the system under delay constraints, especially for Rayleigh fast fading and Rayleigh block fading channels. Meanwhile, simulations in a 2-dimension Poisson network are provided to verify the theoretical results about the lower bounds of the energy–delay tradeoff and the energy efficiency.

Furthermore, the applications of the lower bound of the energy–delay tradeoff were presented. A parameter optimization process is proposed to adjust the parameters from both physical and protocol layers for applications with or without delay constraint.

References

[1] K. Jaffres-Runser, J.M. Gorce, S. Ubeda, Multiobjective qos-oriented planning for indoor wireless lans, in: Proceedings of the 64th IEEE Vehicular Technology Conference (VTC'06-Fall), 2006, pp. 1–5.
[2] M. Haenggi, On routing in random rayleigh fading networks, IEEE Transactions on Wireless Communications 4 (4) (2005) 1553–1562.
[3] M. Haenggi, D. Puccinelli, Routing in ad hoc networks: a case for long hops, IEEE Communications Magazine 43 (10) (2005) 93–101.
[4] P. Chen, B. O'Dea, E. Callaway, Energy efficient system design with optimum transmission range for wireless ad hoc networks, in: Proceedings of IEEE International Conference on Communications (ICC'02), vol. 2, 2002, pp. 945–952.
[5] J.L. Gao, Analysis of Energy Consumption for Ad Hoc Wireless Sensor Networks Using a Bit-meter-per-joule Metric, Jet Propulsion Laboratory, California Institute of Technology, Tech. Rep. 42-150, 2002.
[6] J. Deng, Y.S. Han, P.N. Chen, P.K. Varshney, Optimal transmission range for wireless ad hoc networks based on energy efficiency, IEEE Transactions on Communications 55 (7) (2007) 1439.
[7] S. Cui, R. Madan, A.J. Goldsmith, S. Lall, Cross-layer energy and delay optimization in small-scale sensor networks, IEEE Transactions on Wireless Communications 6 (10) (2007) 3688–3699.
[8] D. Ganesan, B. Krishnamachari, A. Woo, D. Culler, D. Estrin, S. Wicker, Complex Behavior at Scale: An Experimental Study of Low-power Wireless Sensor Networks, UCLA, Tech. Rep. CS TR 02-0013, 2003.
[9] A. Woo, D.E. Culler, Evaluation of Efficient Link Reliability Estimators for Low-power Wireless Networks, Computer Science Division, University of California, Tech. Rep., 2003.
[10] J. Zhao, R. Govindan, Understanding packet delivery performance in dense wireless networks, in: Proceedings of the 1st International Conference on Embedded Networked Sensor Systems, ACM Press, Los Angeles, California, USA, 2003, pp. 1–13.
[11] M.Z. Zamalloa, K. Bhaskar, An analysis of unreliability and asymmetry in low-power wireless links, ACM Transactions on Sensor Networks 3 (2) (2007) 7.
[12] J.-M. Gorce, R. Zhang, H. Parvery, Impact of radio link unreliability on the connectivity of wireless sensor networks, EURASIP Journal on Wireless Communications and Networking (2007) 1–15 (Article ID 19196).
[13] S. Karim, Z. Marco, H. Ahmed, K. Bhaskar, Energy-efficient forwarding strategies for geographic routing in lossy wireless sensor networks, in: Proceedings of The 2nd International Conference on Embedded Networked Sensor Systems, Baltimore, MD, USA, ACM, 2004, pp. 108–121.
[14] R. Zhang, J.-M. Gorce, O. Berder, O. Sentieys, Lower bound of energy–latency tradeoff of opportunistic routing in multihop networks, EURASIP Journal on Wireless Communications and Networking (2011) (Article ID 265083).
[15] H. Karl, A. Willig, Protocols and Architectures for Wireless Sensor Networks, John Wiley and Sons, 2005.
[16] Micaz Datasheet. <www.xbow.com>.
[17] R. Zhang, J.M. Gorce, K. Jaffrès-Runser, Energy–delay Bounds Analysis in Wireless Multi-hop Networks with Unreliable Radio Links, ARES/ INRIA, Tech. Rep. 6598, 2008.
[18] M. Haenggi, The impact of power amplifier characteristics on routing in random wireless networks, in: Proceedings of IEEE Global Telecommunications Conference (GLOBECOM'03), vol. 1, 2003, pp. 513–517.
[19] R. Corless, G. Gonnet, D. Hare, D. Jeffrey, D. Knuth, On the Lambert W function, Advances in Computational Mathematics 5 (1) (1996) 329–359.
[20] A. Ravindran, K.M. Ragsdell, G.V. Reklaitis, Engineering Optimization, second ed., Wiley, 2006.
[21] S. Cui, R. Madan, A. Goldsmith, S. Lall, Joint routing, MAC, and link layer optimization in sensor networks with energy constraints, in: Proceedings of IEEE International Conference on Communications (ICC'05), vol. 2, 2005, pp. 725–729.
[22] <http://wsnet.gforge.inria.fr/>.
[23] G.G. Finn, Routing and Addressing Problems in Large Metropolitan-scale Internetworks, University of Southern California, Marina del Rey. Information Sciences Inst., Tech. Rep., 1987.
[24] M. Haenggi, On distances in uniformly random networks, IEEE Transactions on Information Theory 51 (10) (2005) 3584–3586.
[25] L.E. Miller, Distribution of link distances in a wireless network, Journal of Research of the National Institute of Standards and Technology 106 (2001) 401–412.
[26] C. Rose, Mean internodal distance in regular and random multihop networks, IEEE Transactions on Communications 40 (8) (1992) 1310–1318.

Ruifeng Zhang received the B.S. degree in Electronics Engineering from Taiyuan University of Science and Technology, China, in 1999, and the M.S. degree in Electronics Engineering from Shanghai University, China, in 2003, and the Ph.D. degree in Information from Institue National des sciences appliquées (INSA) de Lyon, France, in 2009. His research interests include wireless communications, cooperative opportunistic communications, wireless sensor networks and multiple-antenna wireless communication systems and networks.

Olivier Berder received the B.S., M.S., and Ph.D. degrees in electrical engineering from the University of Bretagne Occidentale, Brest, in 1998, 1999, and 2002, respectively. From 2002 to 2004 he was with the Laboratory for Electronics and Telecommunication Systems (LEST-UMR CNRS 6165), Brest. From October 2004 to February 2005 he was with the Speech and Sound Technologies and Processes Laboratory in FT R&D, Lannion, France. In March 2005 he joined ENSSAT Lannion at the University of Rennes 1 where is currently an Assistant Professor, and the laboratory IRISA in Rennes. His research interests focus on multiantenna systems and cooperative techniques for mobile communications and wireless sensor networks.

Jean-Marie Gorce received the Dipl. Ing. (M.Sc.) degree in electrical engineering (1993) and the Ph.D. degree (1998) from INSA Lyon. He joined the Telecommunications Department at INSA Lyon in 1998. Since 2001 he is also a member of INRIA. From 2009 He is leading the team Swing (Smart Wireless Networking). He is the Director of CITI (Centre for Innovation in Telecommunications and Integration of Services). His main research fields concern wireless communications focusing on realistic modeling, wireless system optimization and performance assessment considering both infrastructure-based and ad hoc networks. He has published over 80 refereed journal and conference papers (e.g., IEEE Ant & Propag, IEEE TWC, IEEE Wireless Com, IEEE Com. Lett., etc). He serves as an evaluator for several projects for the French national research agency (ANR), and other international organizations like EPSRC (Engineering and Physical Science Research Council). He was TPC member of various conferences (PIMRC 2008, VTC 2008, 2009). He is an Associate Editor of Telecommunication Systems (Springer).

Olivier Sentieys joined University of Rennes (ENSSAT) and IRISA Laboratory, France, as a full Professor of Electronics Engineering, in 2002. He is leading the CAIRN Research Team common to INRIA Institute (national institute for research in computer science and control) and IRISA Lab. (research institute in computer science and random systems). His research activities are in the two complementary fields of embedded systems and signal processing. Roughly, he works firstly on the definition of new system-on-chip architectures, especially the paradigm of reconfigurable systems, and their associated CAD tools, and secondly on some aspects of signal processing like finite arithmetic effects and cooperation in mobile systems. He is the author or coauthor of more than 150 journal publications or peer-reviewed conference papers and holds five patents.